The ESO slice project (ESP) galaxy redshift survey VI. Groups of galaxies

S. Maurogordato

Astron. Astrophys. 342, 1–14 (1999)

ASTRONOMY AND ASTROPHYSICS

The ESO slice project (ESP) galaxy redshift survey⋆,⋆⋆

VI. Groups of galaxies

M. Ramella[1], G. Zamorani[2,3], E. Zucca[2,3], G.M. Stirpe[2], G. Vettolani[3], C. Balkowski[4], A. Blanchard[5], A. Cappi[2], V. Cayatte[4], G. Chincarini[6,7], C. Collins[8], L. Guzzo[6], H. MacGillivray[9], D. Maccagni[10], S. Maurogordato[11,4], R. Merighi[2], M. Mignoli[2], A. Pisani[1], D. Proust[4], and R. Scaramella[12]

[1] Osservatorio Astronomico di Trieste, via Tiepolo 11, I-34131 Trieste, Italy
[2] Osservatorio Astronomico di Bologna, via Zamboni 33, I-40126 Bologna, Italy
[3] Istituto di Radioastronomia del CNR, via Gobetti 101, I-40129 Bologna, Italy
[4] Observatoire de Paris, DAEC, Unité associée au CNRS, D0173 et à l'Université Paris 7, 5 Place J. Janssen, F-92195 Meudon, France
[5] Université L. Pasteur, Observatoire Astronomique, 11 rue de l'Université, F-67000 Strasbourg, France
[6] Osservatorio Astronomico di Brera, via Bianchi 46, I-22055 Merate (LC), Italy
[7] Università degli Studi di Milano, via Celoria 16, I-20133 Milano, Italy
[8] Astrophysics Research Institute, Liverpool John-Moores University, Byrom Street, Liverpool L3 3AF, UK
[9] Royal Observatory Edinburgh, Blackford Hill, Edinburgh EH9 3HJ, UK
[10] Istituto di Fisica Cosmica e Tecnologie Relative, via Bassini 15, I-20133 Milano, Italy
[11] CERGA, Observatoire de la Côte d'Azur, B.P. 229, F-06304 Nice Cedex 4, France
[12] Osservatorio Astronomico di Roma, via Osservatorio 2, I-00040 Monteporzio Catone (RM), Italy

Received 15 July 1998 / Accepted 27 October 1998

Abstract. In this paper we identify objectively and analyze groups of galaxies in the recently completed ESP survey ($23^h23^m \leq \alpha_{1950} \leq 01^h20^m$ and $22^h30^m \leq \alpha_{1950} \leq 22^h52^m$; $-40^o45' \leq \delta_{1950} \leq -39^o45'$). We find 231 groups above the number overdensity threshold $\delta\rho/\rho$ =80 in the redshift range 5000 km s^{-1} $\leq cz \leq$ 60000 km s^{-1}. These groups contain 1250 members, 40.5% of the 3085 ESP galaxies within the same cz range.

The median velocity dispersion (corrected for measurement errors and computed at the redshift of the group) is $\sigma_{ESP,median}$ = 194 km s^{-1}. We show that our result is reliable in spite of the particular geometry of the ESP survey (two rows of tangent circular fields of radius $\theta = 15$ arcmin), which causes most systems to be only partially surveyed. In general, we find that the properties of ESP groups are consistent with those of groups in shallower (and wider) catalogs (e.g. CfA2N and SSRS2). As in shallower catalogs, ESP groups trace very well the geometry of the large scale structure. Our results are of particular interest because the depth of the ESP survey allows us to sample group properties over a large number of structures.

We also compare luminosity function and spectral properties of galaxies that are members of groups with those of isolated galaxies. We find that galaxies in groups have a brighter M^* with respect to non–member galaxies; the slope α is the same, within the errors, in the two cases. We find that 34% (467/1360) of ESP galaxies with detectable emission lines are members of groups. The fraction of galaxies without detectable emission lines in groups is significantly higher: 45% (783/1725). More generally, we find a gradual decrease of the fraction of emission line galaxies among members of systems of increasing richness. This result confirms that the morphology-density relation found for clusters also extends toward systems of lower density.

Key words: galaxies: clusters: general – galaxies: distances and redshifts – galaxies: luminosity function, mass function – cosmology: observations – cosmology: large-scale structure of Universe

1. Introduction

The study of groups of galaxies as dynamical systems is interesting not only *per se*, but also because groups can be used to set constraints on cosmological models (e.g. Frenk et al. 1990; Weinberg & Cole 1992, Zabludoff et al. 1993; Zabludoff & Geller 1994, Nolthenius et al. 1994, 1997) and on models of galaxy formation (Frenk et al. 1996; Kaufmann et al. 1997). Groups are also interesting sites where to look for interactions of galaxies with their environment, in order to obtain information on galaxy evolution processes (Postman & Geller 1984, Allington-Smith et al. 1993).

Group catalogs identified in redshift space are increasing both in number and size (CfA2N, RPG; SSRS2, Ramella et al. 1998; Perseus-Pisces, Trasarti Battistoni 1998; LCRS, Tucker et al. 1997). At the same time, cosmological n-body simulations

Send offprint requests to: Massimo Ramella (ramella@oat.ts.astro.it)

⋆ based on observations collected at the European Southern Observatory, La Silla, Chile.

⋆⋆ Table 1 is available only in electronic form via anonymous ftp to cdsarc.u-strasbg.fr (130.79.128.5) or via http://cdsweb.u-strasbg.fr/Abstract.html

are reaching the resolution required to allow replication of the observational techniques for the identification of groups. In particular, Frederic (1995a,b) uses n-body simulations to evaluate and compare the performances of commonly used group finding algorithms.

Among the main properties of groups, the velocity dispersion is of particular interest. It is easy to measure and it is well suited for comparison with the predictions of cosmological n-body models (Frenk et al. 1990; Moore et al. 1993; Zabludoff et al. 1993). Distributions of velocity dispersions of nearby groups are now well determined with rather small statistical uncertainties given the large size of the samples. Ramella et al. 1995 and Ramella et al. 1996 survey the redshifts of candidate faint members of a selection of nearby groups and find that the velocity dispersion of groups is stable against inclusion of fainter members. In other words, the velocity dispersion estimated on the basis of the fewer original bright members is a good indicator of the velocity dispersion obtained from a better sampling of the same group.

In this paper we identify and analyze groups of galaxies in the recently completed ESP survey (Vettolani et al. 1997). The ESP group catalog is interesting because of its depth ($b_J \leq 19.4$) and because it samples a new independent region of the universe. ESP is a nearly bi-dimensional survey (the declination range is much smaller than the right ascension range), five times deeper than either CfA2 (Geller & Huchra 1989) or SSRS2 (da Costa et al. 1994). The volume of the survey is $\sim 5 \times 10^4\ h^{-3}\,\mathrm{Mpc}^3$ at the sensitivity peak of the survey, $z \sim 0.1$, and $\sim 1.9 \times 10^5\ h^{-3}\,\mathrm{Mpc}^3$ at the effective depth of the sample, $z \sim 0.16$. Even if the volume of ESP is of the same order of magnitude of the volumes explored with the individual CfA2, SSRS2, and Perseus-Pisces samples, it intercepts a larger number of structures. In fact, the strip geometry is very efficient for the detection of large scale structures within redshift surveys (de Lapparent et al. 1988).

In particular we determine the distribution of the velocity dispersions of groups and show that our result is reliable in spite of the particular geometry of the ESP survey (two rows of adjacent circular fields of radius $\theta = 16$ arcmin, see Fig. 1 of Vettolani et al. 1997).

An important aspect that distinguishes the ESP group catalog from the other shallower catalogs is that we have the spectra of all galaxies with measured redshift. It is already well known that emission line galaxies are rarer in rich clusters than in the field (Biviano et al. 1997). The relation between the fraction of emission line galaxies and the local density is a manifestation of the morphology–density relationship observed for clusters (Dressler 1980), a useful tool in the study of galaxy evolution. With the ESP catalog we explore the extent of the morphology density relationship in the intermediate range of densities that are typical of groups at a larger depth than in previous studies.

We note that preliminary results of a search for groups in the Las Campanas Redshift Survey (Shectman et al. 1996) have been presented by Tucker et al. (1997). The properties of these groups, as distant as ours, are difficult to compare with those of our ESP groups and with those of shallower surveys because LCRS a) is a red band survey (ESP and shallower surveys are selected in the blue band), b) it is not simply magnitude limited, and c) it does not uniformly sample structures in redshift space. In particular, the different selection criteria could have a strong impact on the results concerning the morphology-density relation, the luminosity segregation, and the possible differences between the luminosity functions of member and non-member galaxies.

In Sect. 2 we briefly describe the data; in Sect. 3 we analyze the effect of the ESP geometry on the estimate of the velocity dispersion of groups; in Sect. 4 we summarize the group identification procedure; in Sect. 5 we present the ESP group catalog; in Sect. 6 we analyze properties of groups that are relevant to a characterization of the Large Scale Structure (LSS); in Sect. 7 we analyze the properties of galaxies in groups and compare them to the properties of "field" galaxies (*i.e.* galaxies that have not been assigned to groups) and "cluster" galaxies; in Sect. 8 we identify ESP counterparts of ACO and/or EDCC clusters (Lumsden et al. 1992). Finally, we summarize our results in Sect. 9.

2. The data

The ESO Slice Project (ESP) galaxy redshift survey is described in Vettolani et al. (1997). The data of the full sample together with a detailed description of the instrumental set-up and of the data reduction can be found in Vettolani et al. (1998). Here we only briefly describe the survey.

The ESP survey extends over a strip of $\alpha \times \delta = 22^o \times 1^o$ (strip A), plus a nearby area of $5^o \times 1^o$ (strip B), five degrees West of the main strip, in the South Galactic Pole region ($23^h23^m \leq \alpha_{1950} \leq 01^h20^m$ and $22^h30^m \leq \alpha_{1950} \leq 22^h52^m$ respectively; $-40^o45' \leq \delta_{1950} \leq -39^o45'$). Each of the two strips is covered with two rows of slightly overlapping circular fields of angular radius $\theta = 16$ arcmin, the separation between the centers of neighboring circles being 30 arcmin. Each field corresponds to the field of view of the multifiber spectrograph OPTOPUS at the 3.6m ESO telescope that was used to obtain almost all of the spectra (the MEFOS spectrograph was used in the last ESP run). Throughout this paper we will assume that the circular fields are tangent, with an angular radius of 15 arcmin: this simplification has no consequences on the galaxy sample. The total solid angle of the spectroscopic survey is 23.2 square degrees.

The galaxy catalog consists of all (candidate) galaxies brighter than the limiting magnitude $b_{J,lim} = 19.4$ listed in the Edinburgh–Durham Southern Galaxy Catalogue (Heydon–Dumbleton et al. 1988, 1989).

The spectra cover the wavelength range 3730Å to 6050Å, with an average pixel size of 4.5Å. Galaxy redshifts are measured by cross–correlating sky-subtracted spectra with a set of 8 template stars observed with the same instrumental set-up used to obtain the galaxy spectra. In this paper we use emission line redshifts only for galaxies with no reliable absorption line redshift. The median internal velocity error is of the order of $\sim 60\,\mathrm{km\,s^{-1}}$. From a comparison of our 8 templates with

three SAO radial velocity standard stars we estimate that the zero–point error should be smaller than $\sim 10\,\mathrm{km\,s^{-1}}$.

The total number of confirmed galaxies with reliable redshift measurement is 3342. The completeness of strip A and strip B are estimated to be 91% and 67% respectively.

3. ESP geometry and the measure of velocity dispersions

To all practical purposes, the projection of the ESP survey on the sky consists of two rows of adjacent circular OPTOPUS fields of radius 15 arcmin and a separation of 30 arcmin between adjacent centers. The angular extent of groups and clusters at the typical depth of the survey ($z \simeq 0.1$) are comparable, or even larger, than the size of the OPTOPUS fields. Therefore, most systems falling into the survey's volume are only partially surveyed.

The main effect of the "mask" of OPTOPUS fields is to hide a fraction of group members that lie within or close to the strip containing the mask (the OPTOPUS fields cover 78% of the area of the "un-masked" strip). Because of the hidden members, several poor groups may not appear at all in our catalog. On the contrary, our catalog might include parts of groups that are centered outside the ESP strip. These problems notwithstanding, we expect to derive useful information on the most important physical parameter of groups, the velocity dispersion, σ_{cz}.

Our estimate of the parent velocity dispersion, σ_p, is based upon the sample standard deviation $\sigma_{cz}(N_{mem})$. The sample standard deviation defined as $\sigma_{cz}(N_{mem}) = \sqrt{\Sigma_i (cz_i - \langle cz \rangle)^2/(N_{mem} - 3/2)}$ is a nearly unbiased estimate of the velocity dispersion (Ledermann, 1984), independent of the size N_{mem} of the sample. We make the standard assumptions that a) barycentric velocities of members are not correlated with their real 3D positions within groups, and that b) in each group the distribution of barycentric velocities is approximately gaussian. Because the position on the sky of the OPTOPUS mask is not related to the positions of groups, its only effect is to reduce at random N_{mem}. Therefore, using an unbiased estimate of the velocity dispersion, the mask has no effect on our determination of the average velocity dispersions of groups.

The effect of the mask is to broaden the distribution of the sample standard deviations. The variance of the distribution of sample standard deviations varies with N_{mem} approximately as $\sigma_{cz}^2/2N_{mem}$ (Ledermann, 1984). This distribution, proportional to the χ^2 distribution, is skewed: even if the mean of the distribution is unbiased, σ_{cz} is more frequently underestimated than overestimated.

While it is easy to predict the effect of the mask on the determination of the velocity dispersion of a single group, it is rather difficult to predict the effect of the mask on the observed distribution of velocity dispersions of a sample of groups with different "true" velocity dispersions and different number of members. In order to estimate qualitatively the effect of the mask on the shape of the distribution of velocity dispersions, we perform a simple Monte Carlo simulation.

We simulate a group by placing uniformly at random N_{mem} points within a circle of angular radius θ_{gr} corresponding, at the redshift of the group, to the linear projected radius R_{gr} = 0.5 h^{-1} Mpc. This radius is the typical size of groups observed in shallow surveys (e.g. RPG). We select the redshift of the group, z_{gr}, by random sampling the observed distribution of ESP galaxy redshifts.

In order to start from reasonably realistic distributions, we set N_{mem} and the velocity dispersion, σ_{cz}, by random sampling the relative histograms obtained from our ESP catalog. We limit the range of N_{mem} to $3 \leq N_{mem} \leq 18$ and the range of σ_{cz} to $0 \leq \sigma_{cz} \leq 1000\,\mathrm{km\,s^{-1}}$.

We lay down at random the center of the simulated group within the region of the sky defined by extending 15 arcmin northward and southward the "un-masked" limits of the ESP survey. We then assign to each of the N_{mem} points a barycentric velocity randomly sampled from a gaussian with dispersion σ_{cz} centered on z_{gr}. We compute the velocity dispersion, $\sigma_{no-mask}$, of the N_{mem} velocities. Finally, we apply the mask and discard the points that fall outside the mask. We discard the whole group if there are fewer than 3 points left within the mask ($N_{mem,mask} < 3$). If the group "survives" the mask, we compute the dispersion σ_{mask} of the $N_{mem,mask}$ members. On average, 78% of the groups survive the mask (this fraction corresponds to the ratio between the area covered by the mask and the area of the "un-masked" strip). The percentage of surviving groups depends on the exact limits of the region where we lay down at random groups and on the projected distribution of members within R_{gr}. For the purpose of the simulation, the fraction of surviving groups is not critical.

We repeat the procedure 100 times for n_{gr} = 231 simulated groups (the number of groups identified within ESP). At each run we compute the histograms N($N_{mem,mask}$) and N(σ_{mask}).

In Fig. 1 we plot the input distribution N(N_{mem}) – thin line– together with the average output distribution, $\langle \mathrm{N}(N_{mem,mask}) \rangle n_{gr}/n_{mask}$ – thick line–. Errorbars represent $\pm$ one standard deviation derived in each bin from the distribution of the 100 histograms N($N_{mem,mask}$); for clarity we omit the similar errorbars of N(N_{mem}. The factor n_{gr}/n_{mask} normalizes the output distribution to the number of input groups. The two histograms in Fig. 1 are clearly very similar since N(N_{mem}) is within one sigma from $\langle \mathrm{N}(N_{mem,mask}) \rangle n_{gr}/n_{mask}$ for all values of N_{mem}. We point out here that the similarity between the input and output histograms does not mean that the surviving groups have not changed. In fact only about 63% of the triplets survive the mask while, for example, 88% of the groups with 5 members and 98% of those with 10 members "survive" the mask.

Fig. 2 shows the results of our simple simulation for the velocity dispersion. The thin histogram is the input "true" distribution N(σ_{gr}). The dotted histogram is the average "observed" distribution obtained without dropping galaxies that lie outside the OPTOPUS mask, N($\sigma_{no-mask}$). This is the distribution we would observe if the geometry of the survey would be a simple strip. The third histogram (thick line) is the average output distribution in presence of the OPTOPUS mask, $\langle \mathrm{N}(\sigma_{mask}) \rangle n_{gr}/n_{mask}$ (errorbars are $\pm$ one-sigma). The input distribution N(σ_{gr}), the distribution N($\sigma_{no-mask}$), and the

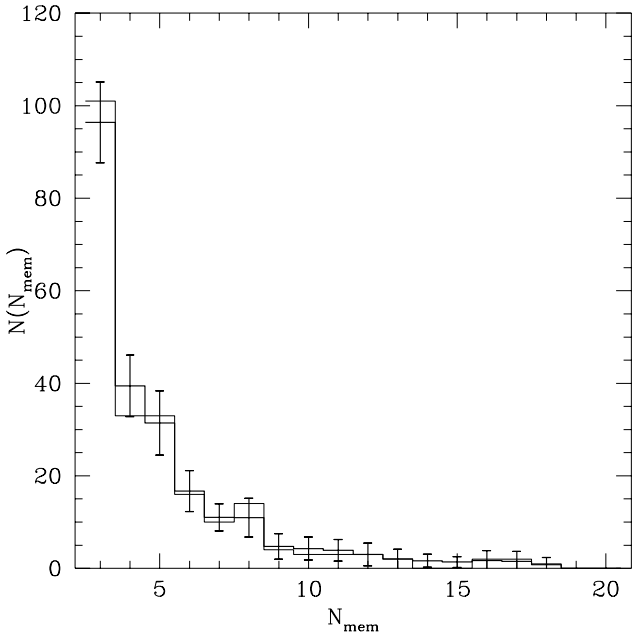

Fig. 1. Effect of the "OPTOPUS mask" on N(N_{mem}): the thin histogram is the "true" distribution, the thick histogram is the average distribution "observed" through the "OPTOPUS mask", normalized to the number of input groups. Errorbars represent $\pm$ one standard deviation.

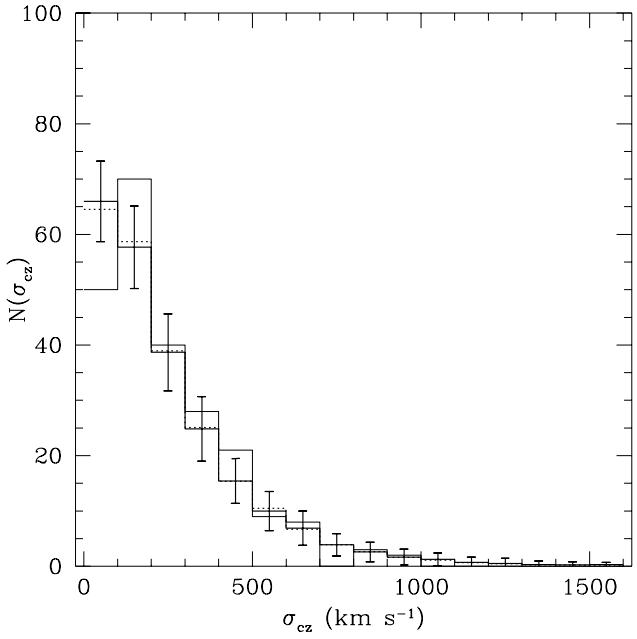

Fig. 2. Effect of the "OPTOPUS mask" on N(σ_{gr}). The thin histogram is the "real" distribution, the dotted histogram shows the effect of sampling on the input distribution, and the thick histogram is the average distribution "observed" through the "OPTOPUS mask", normalized to the number of input groups. Errorbars represent $\pm$ one standard deviation.

distribution $\langle \mathrm{N}(\sigma_{mask})\rangle n_{gr}/n_{mask}$ are all within one-sigma from each other. In particular the two distributions we observe with and without OPTOPUS mask are undistinguishable (at the 99.9% confidence level, according to the KS test). The low velocity dispersion bins are slightly more populated in the "observed" histograms because the estimate of the "true" σ_{cz} is based on small N_{mem}. Note that in the case of real observations, some groups in the lowest σ_{cz} bin will be shifted again to the next higher bin because of measurement errors.

Our results do not change if we take into account the slight dependence of σ_{cz} from N_{mem} observed within our ESP catalog: also in this case the effect of the mask is negligible.

In conclusion, the simulation confirms our expectation that the OPTOPUS mask has no significant effect on the shape of the distribution of velocity dispersions.

4. Group identification

We identify groups with the so-called friend-of-friend algorithm (FOFA; Huchra & Geller, 1982) as described in RPG. We implement here the cosmological corrections required by the depth of the sample ($z \leq 0.2$). Throughout this paper we use H_o = 100 km s^{-1} Mpc^{-1} and $q_0 = 0.5$.

For each galaxy in the magnitude limited ESP catalog, the FOFA identifies all other galaxies with a projected comoving separation

$$D_{12} \leq D_L(V_1, V_2) \tag{1}$$

and a line-of-sight velocity difference

$$V_{12} \leq V_L(V_1, V_2). \tag{2}$$

Here $V_1 = cz_1$ and $V_2 = cz_2$ are the velocities of the two galaxies in the pair. All pairs linked by a common galaxy form a "group".

The two parameters D_L, V_L are scaled with distance in order to take into account the decrease of the magnitude range of the luminosity function sampled at increasing distance. The scaling is

$$D_L = D_o R \tag{3}$$

and

$$V_L = V_o R, \tag{4}$$

where

$$R = \left[\int_{-\infty}^{M_{lim}} \Phi(M) dM \Big/ \int_{-\infty}^{M_{12}} \Phi(M) dM \right]^{1/3}, \tag{5}$$

$$M_{12} = b_{J,lim} - 25 - 5\log(d_L(\bar{z}_{12})) - \langle K(\bar{z}_{12}) \rangle, \tag{6}$$

and M_{lim} is the absolute magnitude corresponding to $b_{J,lim}$ at a fiducial velocity V_f. We compute $d_L(\bar{z}_{12})$ with the Mattig (1958) expression, where $\bar{z}_{12} = .5(z_1 + z_2)$. Finally, $\langle K(\bar{z}_{12}) \rangle$ is the $K-$correction "weighted" with the expected morphological mix at each redshift as in Zucca et al. (1997).

The scaling is the same for both D_L and V_L and it is normalized at the fiducial velocity V_f = 5000 km s^{-1}, where D_0 = $D_L(V_f)$ and V_0 = $V_L(V_f)$. In particular, a given value of D_0 corresponds to a minimum number overdensity threshold for groups, $\delta\rho/\rho$. The luminosity function we use is the

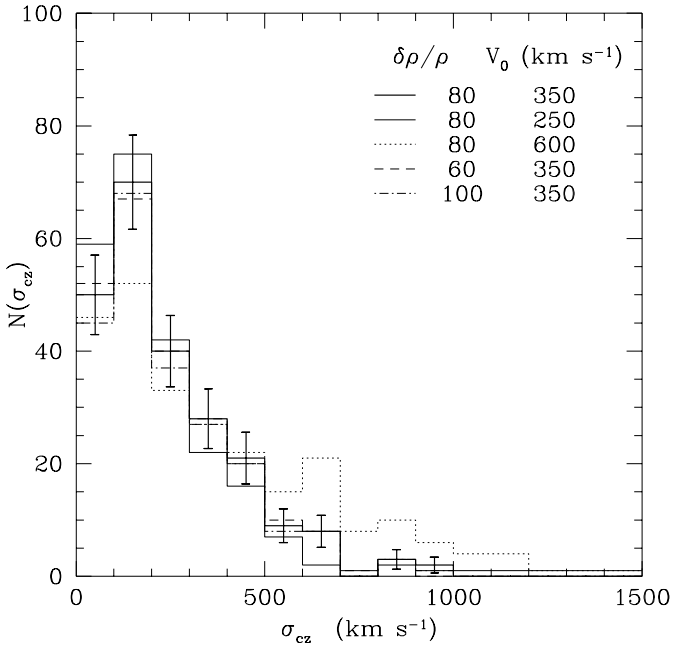

Fig. 3. The distribution of velocity dispersions, N(σ_{cz}), of different ESP group catalogs obtained for a grid of values of the search parameters $\delta\rho/\rho$ and V_0. Errorbars represent $\pm$ one standard deviation.

Schechter parametrization with $M^* = -19.61$, $\alpha = -1.22$, and $\phi^* = 0.020\,\mathrm{Mpc}^{-3}$ computed for ESP galaxies by Zucca et al. (1997).

We do not consider galaxies with velocities $cz \leq V_f$ because the linear extension of the survey in the direction of the declination is smaller than the typical size of a group for $cz \leq$5000 km s^{-1}. We also limit the maximum depth of our group catalog to $cz \leq 60000\,\mathrm{km\,s^{-1}}$. Beyond this limit the accessible part of the luminosity function becomes very small and the scaling of the FOFA linking parameters excessively large.

The main characteristics of the distribution of galaxies within the volume of the universe surveyed by ESP (Vettolani et al. 1997) are very similar to those observed within shallower, wider angle magnitude limited redshift surveys. For this reason we expect that the conclusions on the fine-tuning of FOFA reached by Ramella et al. 1989, Frederic 1995a, and RPG will hold true also for ESP. In particular, RPG show that within the CfAN2 redshift survey the choice of the FOFA parameters is not critical in a wide region of the parameter space around ($\delta\rho/\rho$ = 80, V_0 = 350 km s^{-1}). With our luminosity function and fiducial velocity, we obtain $\delta\rho/\rho$ = 80 for D_0 = 0.26 Mpc, a value comparable to the D_0 value used for CfAN2. It is therefore reasonable to expect that the same results of the exploration of the parameter space will hold also for the ESP survey. In order to verify our expectation, we run FOFA with the following five pairs of values of the linking parameters selected among those used by RPG: ($\delta\rho/\rho$ = 80, V_0 = 250 km s^{-1}), ($\delta\rho/\rho$ = 80, V_0 = 350 km s^{-1}), ($\delta\rho/\rho$ = 80, V_0 = 600 km s^{-1}), ($\delta\rho/\rho$ = 60, V_0 = 350 km s^{-1}), ($\delta\rho/\rho$ = 100, V_0 = 350 km s^{-1}). Based on RPG, these pairs of values are sufficient to give an indication of the stability of the group catalogs in the parameter space (D_L,V_L). The number of groups in the five cases is N_{groups} = 217, 231, 253, 239, and 217 respectively.

We plot in Fig. 3 the observed distributions of the velocity dispersions of the five group catalogs. We compare the distribution obtained for ($\delta\rho/\rho$ = 80, V_0 = 350 km s^{-1}) –thick histogram in Fig. 3 – with the other four distributions and find that the only significant difference (99.9% level, according to the KS test) occurs with the distribution obtained using the largest velocity link, V_0 = 600 km s^{-1} (dotted histogram). This value of the velocity-link produces an excess of high velocity dispersion systems. Frederic 1995a, Ramella et al. 1989, and RPG argue that these high velocity dispersion systems are likely to include a significant number of interlopers (galaxies with high barycentric velocity that are not physically related to the group in real space).

On the basis of the results of our tests, we choose the catalog obtained with $\delta\rho/\rho$ = 80 (D_0 = 0.26 h^{-1} Mpc) and V_0 = 350 km s^{-1} as our final ESP group catalog. This choice offers the advantage of a straightforward comparison between the properties of ESP catalog and those of the CfA2N (RPG), and SSRS2 (Ramella et al. 1998) catalogs.

5. The group catalog

We identify 231 groups within the redshift limits $5000 \leq cz \leq 60000\,\mathrm{km\,s^{-1}}$. These groups contain 1250 members, 40.5% of the 3085 ESP $b_J \leq 19.4$ galaxies within the same cz range.

In Table 1 we present our group catalog. For each group we list the ID number (column 1), the number of members (column 2), the coordinates α_{1950} and δ_{1950} (columns 3 and 4 respectively), the mean radial velocity cz in km s^{-1} corrected for Virgo infall and galactic rotation (column 5), and the velocity dispersion σ_{cz} (column 6). We compute the velocity dispersion following the prescription of Ledermann (1984) for an unbiased estimator of the dispersion (see previous section). We also take into account the cosmological expansion of the universe and the measurement errors according to the prescriptions of Danese et al. (1980). The errors we associate to the redshifts are those output by the RVSAO cross-correlation procedure multiplied by a factor 1.6. This factor brings the cross-correlation error in rough agreement with the external error estimated from repeated observations (Vettolani et al. 1998 – here we do not distinguish between emission and absorption line redshifts). Table 1 is available only in electronic form via anonymous ftp to cdsarc.u-strasbg.fr (130.79.128.5) or via http://cdsweb.u-strasbg.fr/Abstract.html.

In the case of 24 groups, the correction of σ_{cz} for the measurement errors leads to a negative value. In column 6 of Table 1 we give the error as an upper limit to σ_{cz} for these groups.

Not all galaxies in the region of the sky covered by the ESP survey have a measured redshift. Of the original target list, 444 objects are not observed, and 207 objects have a noisy spectrum, insufficient for a reliable determination of the redshift. In Table 1 we give, for each group, the ratio of these objects to the number of members (column 7). In computing these rates, we assign to each group the objects without redshift whose (α, δ)

coordinates fall within the angular region defined by the union of the N_{mem} circular regions obtained by projecting on the sky circles of linear radius $D_L(cz_{group})$ centered on all group members. There are groups that are separated along the line-of-sight but that overlap once projected on the sky. If an object without redshift lies within the overlap region, we assign the object to both groups.

There are 67 groups that do not contain any object of the photometric catalog without measured redshift. On the other hand, in the case of 51 groups the number of objects without redshift equals, or exceeds, the number of members. These groups are mostly triplets and quadruplets. Only 14 out of the 51 (possibly) highly incomplete groups have $N_{mem} \geq 5$. Most of these groups are located in the relatively small region B of the redshift survey (Vettolani et al. 1998), which is the least complete (completeness level = 71%).

Finally, we estimate that only 8 out of 231 groups are entirely contained within one OPTOPUS field. By "entirely contained" we mean that none of the circles of projected linear radius D_L centered on the member galaxies crosses the edges of the OPTOPUS fields.

6. Properties of groups

In this section we discuss properties of ESP groups that can be used to characterize the LSS and that set useful constraints to the predictions of cosmological N-body models.

6.1. Abundances of groups and members

The first "global" property of groups we consider is the ratio, f_{groups}, of their number to the number of non-member galaxies within the survey. For ESP we have $f_{ESP,groups}$ = 0.13 $\pm$ 0.01, for CfA2N RPG find $f_{CfA2N,groups}$ = 0.13 $\pm$ 0.01, for SSRS2 Ramella et al. 1998 find $f_{SSRS2,groups}$ = 0.12 $\pm$ 0.01. Clearly the proportion of groups among galaxies is the same in all three independent volumes of the universe surveyed with ESP, CfA2N and SSRS2. Because CfA2N and SSRS2 mostly sample only one large structure while ESP intercepts several large structures, our result means that the clustering of galaxies in groups within the large scale structure is homogeneous on scales smaller than those of the structures themselves.

We point out that, on the basis of our simple simulation, we do not expect the OPTOPUS mask to affect the determination of f_{groups}.

We now consider the ratio of member to non-member galaxies, f_{mem}. Within ESP we have $f_{ESP,mem}$ = 0.68 $\pm$ 0.02; within CfAN and SSRS2, the values of the ratio are $f_{CfA2,mem}$ = 0.81 $\pm$ 0.02 and $f_{SSRS2,mem}$ = 0.67 $\pm$ 0.02 respectively. Quoted uncertainties are one poissonian standard deviation. According to the poissonian uncertainties, $f_{ESP,mem}$ and $f_{SSRS2,mem}$ are undistinguishable. The value of $f_{CfA2,mem}$ is significantly different from the other two ratios. However, the real uncertainty in the ratio of members to non-members is higher than the poissonian estimate because the fluctuations in the number of members is dominated by the fluctuations in the smaller number of groups. Moreover, the total number of members is strongly influenced by few very rich systems. In fact, it is sufficient to eliminate two clusters, Virgo and Coma, from CfA2N in order to reduce the value of $f_{CfA2,mem}$ to $f_{CfA2,mem}$ = 0.70 $\pm$ 0.02, in close agreement with the ratio observed within ESP and SSRS2.

In conclusion, groups are a remarkably stable property of the large-scale distribution of galaxies. Once the richest clusters are excluded, the abundances of groups and of members relative to that of non-member or"field" galaxies are constant over several large and independent regions of the universe.

6.2. Distribution of groups in redshift-space

We plot in the top panel of Fig. 4 the cone diagram (α vs cz) for the 3085 ESP galaxies within $5000 < cz < 60000$ km s^{-1}. In the bottom panel of Fig. 4 we plot the cone diagram of the 231 ESP groups. Figs. 4 shows that groups trace very well the galaxy distribution, as they do in shallower surveys ($cz \lesssim 12000$ km s^{-1}). Note that in Fig. 4 we project adjacent beams, not a strip of constant thickness.

The topology of the galaxy distribution in redshift space has already been described by Vettolani et al. (1997) and will be the subject of a forthcoming paper. The most striking features are the voids of sizes $\simeq 50\ h^{-1}$ Mpc and the two density peaks at $cz \simeq 18000$ km s^{-1} and $cz \simeq 30000$ km s^{-1}. These features are also the main features of the group distribution.

In Fig. 5 we plot the redshift distributions of groups (thick histogram) and galaxies (thin galaxies), divided by the total number of groups and by the total number of galaxies, respectively. In Fig. 6 we plot number densities of galaxies in redshift bins. Number densities are computed using the n_3 estimator of Davis & Huchra (1982): all the details about the density estimates are given in Zucca et al. 1997. We vary the size of the redshift bins in order to keep constant the number of galaxies expected in each bin based on the selection function. The top panel is for member galaxies, the middle panel is for isolated and binary galaxies, and the bottom panel is for all ESP galaxies. The dashed lines represent the $\pm$ one sigma corridor around the mean galaxy density.

It is clear from Fig. 5 that the redshift distributions of groups and galaxies are undistinguishable (98% confidence level). Not surprisingly, the number density in redshift bins of members and all galaxies are highly correlated (Fig. 6a and 6c). More interestingly, the number density distribution of non-member galaxies is also correlated with the number density distribution of all galaxies (Fig. 6b and 6c). In particular, the two density peaks at $cz \simeq 18000$ km s^{-1} and $cz \simeq 30000$ km s^{-1} of the number density distribution of all galaxies are also identifiable in the number density distribution of non-member galaxies, even if with a lower contrast.

We know from the previous section that groups are a very stable global property of the galaxy distribution within the volume of the ESP and within other shallower surveys. Here we show that a tight relation between non-member galaxies and groups exists even on smaller scales.

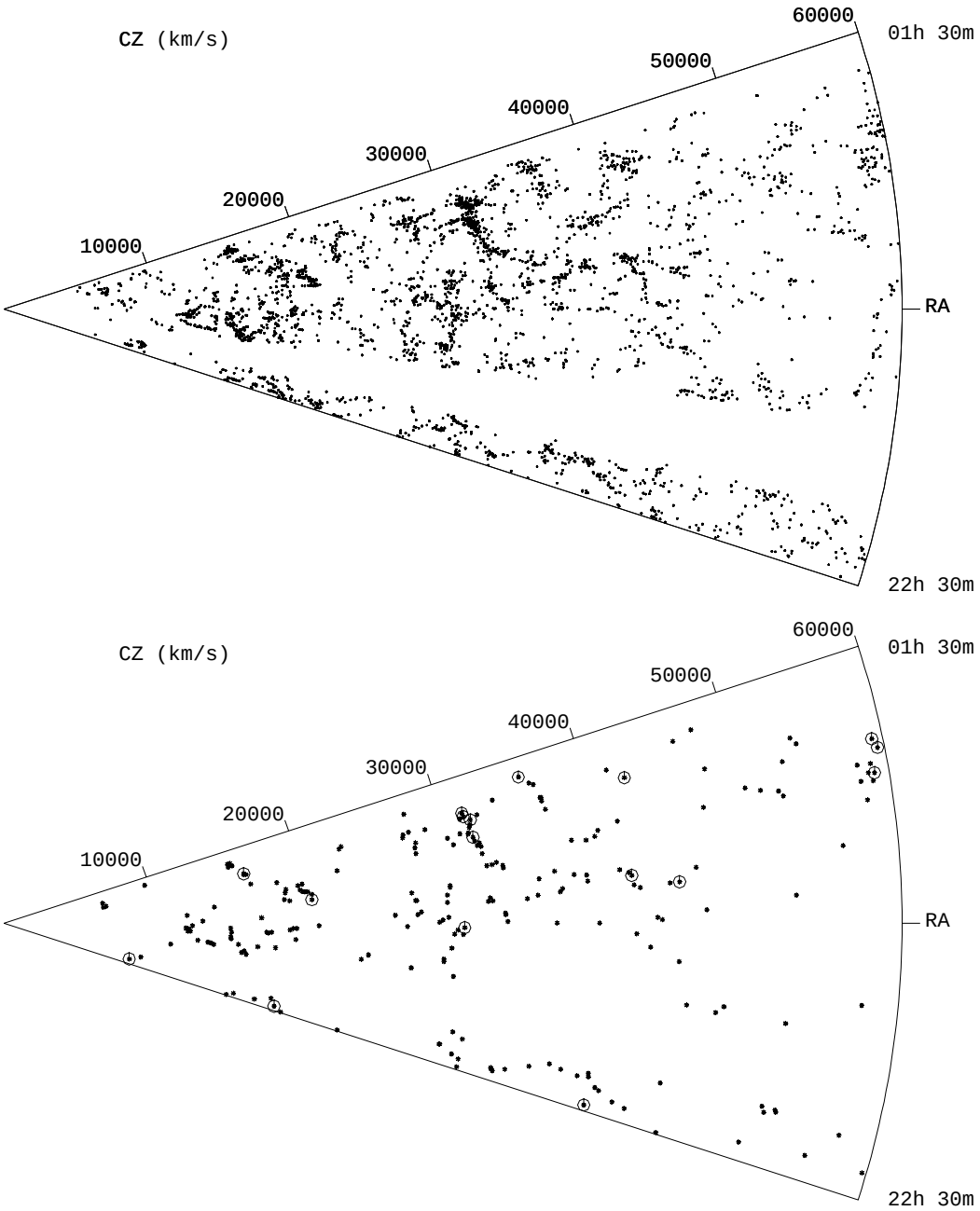

Fig. 4. Cone diagrams (α – cz) of ESP galaxies (*top panel*) and of ESP groups (*bottom panel*). The larger circles in the cone diagram of groups mark the ESP counterparts of known ACO and/or EDCC clusters.

Our result is particularly interesting in view of the depth of the ESP survey and of the number of large structures intercepted along the line-of-sight.

6.3. The distribution of velocity dispersions

We now discuss the velocity dispersions of ESP groups. According to our simulation in Sect. 2, the effect on the velocity dispersions of the OPTOPUS mask is statistically negligible.

The median velocity dispersion of all groups is $\sigma_{ESP,median}$ = 194 (106,339) km s^{-1}. The numbers in parenthesis are the 1st and 3rd quartiles of the distribution. Poor groups with $N_{mem} < 5$ have a median velocity dispersion $\sigma_{median,poor}$=145 (65,254) km s^{-1}, richer groups have $\sigma_{median,rich}$=272 (178,399) km s^{-1}. For comparison, the median velocity dispersions of CfA2N and SSRS2 are $\sigma_{CfA2N,median}$ =198 (88,368) km s^{-1} and $\sigma_{SSRS2,median}$ = 171 (90,289) km s^{-1}. We take the values of the velocity dispersions for the CfA2 and SSRS2 groups from Ramella et al. (1997,1998). In order to compare these velocity dispersions with ours, we correct them for a fixed error of 50 km s^{-1} (corresponding to an RVSAO error of $\simeq$ 35 km s^{-1}) and multiply them by $\sqrt{(N_{mem}-1)/(N_{mem}-3/2)}$. We note that, because of the OPTOPUS mask, the comparison of the velocity dispersions of "rich" and "poor" groups within ESP with those of similar systems within CfA2N and SSRS2 is not meaningful. A fraction of ESP "poor" groups may actually be part of "rich" groups.

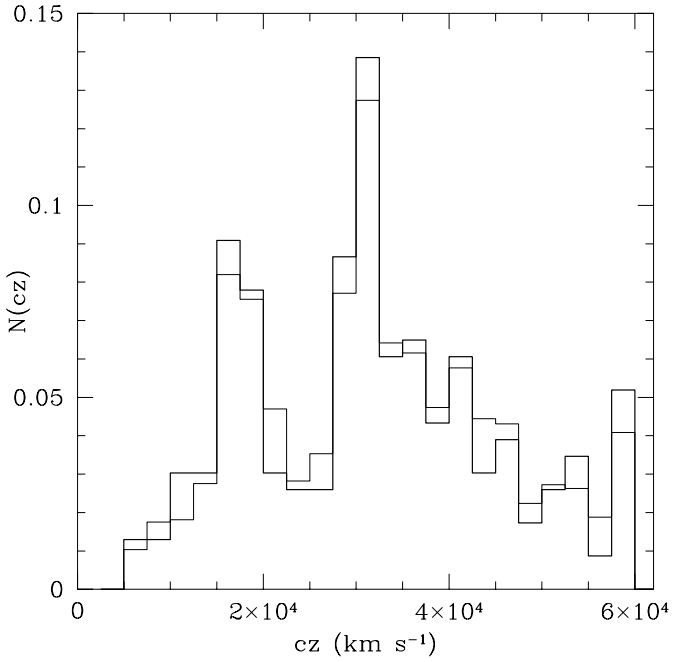

Fig. 5. The redshift distributions of groups (thick histogram) and galaxies (thin histogram), divided by the total number of groups and by the total number of galaxies respectively.

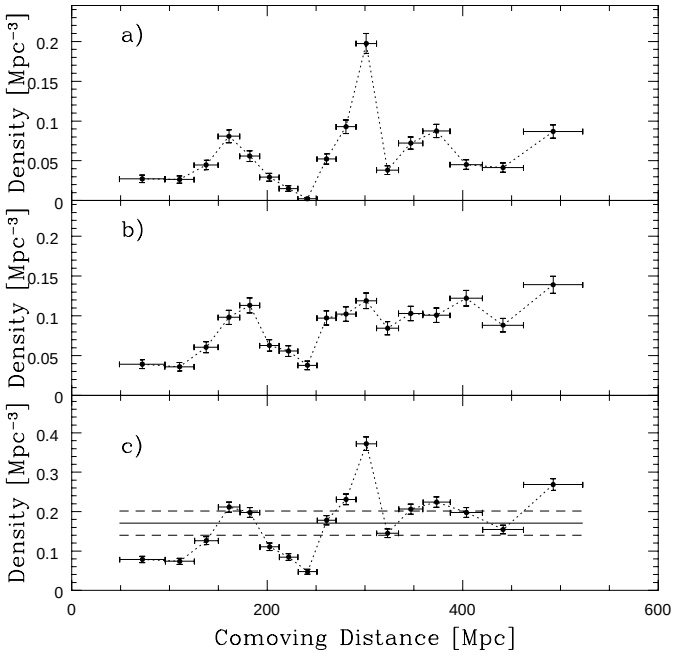

Fig. 6a–c. Number densities of galaxies in comoving distance bins. The *top panel* is for members, the *middle panel* is for non-members, and the *bottom panel* is for all galaxies.The dashed lines represent the $\pm$ one sigma corridor around the mean galaxy density.

In Fig. 7 we plot (thick histogram) the distribution of the velocity dispersions, $n_{ESP}(\sigma)$, normalized to the total number of groups. Errorbars are one sigma poissonian errors. We also plot the normalized σ_{cz} distributions of CfA2N and SSRS2. According to the KS test, differences between $n_{ESP}(\sigma)$ and

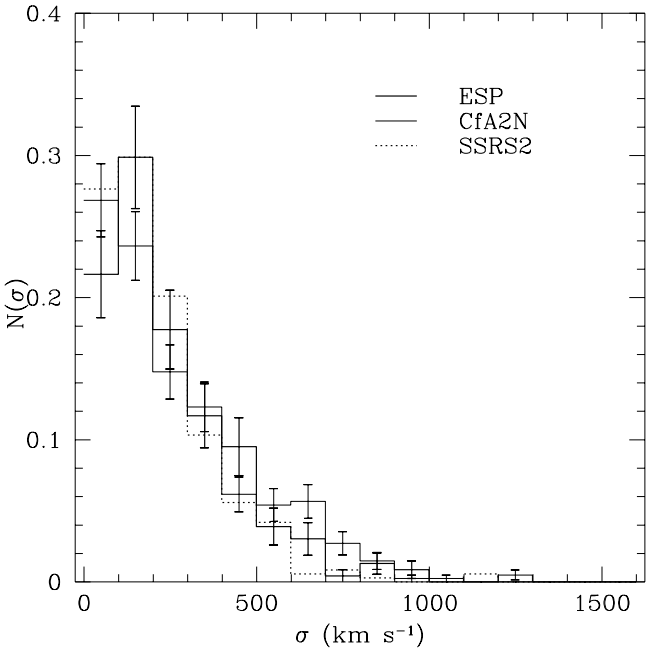

Fig. 7. Comparison between the distribution of velocity dispersions of ESP groups (thick line) and those of CfA2N (thin line) and SSRS2 groups (dotted line). Each distribution is normalized to the total number of groups. Errorbars are one sigma poissonian errors.

the other two distributions are not significant (P_{KS} = 0.3 and 0.2 for the comparison between ESP and CfA2N and SSRS2 respectively).

It is interesting to point out that $n_{CfA2N}(\sigma)$ and $n_{SSRS2}(\sigma)$ do differ significantly (97% level), $n_{CfA2N}(\sigma)$ being richer of high velocity dispersion systems (Marzke et al., 1995). Groups with dispersion velocities $\sigma_{cz} > 700\,\mathrm{km\,s^{-1}}$ are rare and the fluctuations from survey to survey correspondingly high. The abundance of these high σ_{cz} systems is the same within both ESP and SSRS2 (2%) but it is higher within CfA2N (5%). If we disregard these few high velocity dispersion systems, the difference between $n_{CfA2N}(\sigma)$ and $n_{SSRS2}(\sigma)$ ceases to be significant. From this result we conclude that each survey contains a fair representation of groups.

The distribution of velocity dispersions is an important characteristic of groups because it is linked to the group mass. Therefore $n(\sigma)$ constitutes an important constraint for cosmological models. Furthermore, σ_{cz} is a much better parameter for the classification of systems than the number of members (even more so in the case of the present catalog where the OPTOPUS mask affects the number of members much more than velocity dispersions)

The ESP survey provides a new determination of the shape of $n(\sigma)$ in a much deeper volume than those of existing shallower surveys. We find that, within the errors, $n_{ESP}(\sigma)$ is very similar to both $n_{CfA2N}(\sigma)$ and $n_{SSRS2}(\sigma)$.

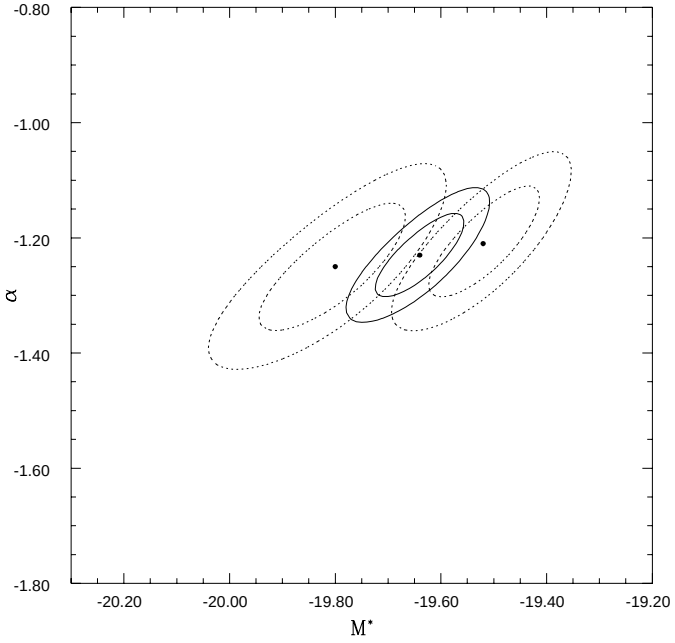

Fig. 8. One- and two-sigma confidence ellipses (dotted lines) of the α and M^* parameters of the Schechter luminosity function of members (brightest M^*) and non-members (faintest M^*). The solid lines show the confidence ellipses derived for the total ESP sample considered in this paper ($5000\,\mathrm{km\,s^{-1}} \leq cz \leq 60000\,\mathrm{km\,s^{-1}}$).

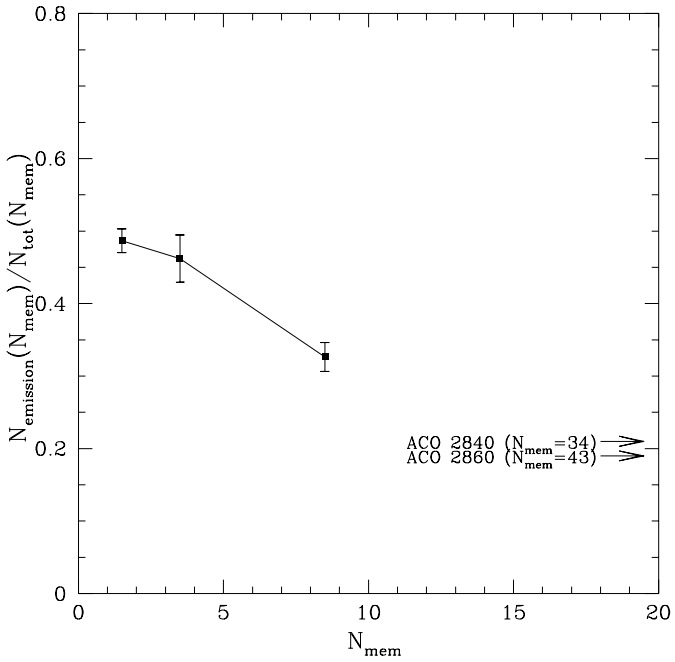

Fig. 9. Fraction of $e.l.$-galaxies in the "field", in poor groups, and rich groups. The two arrows indicate the fraction of $e.l.$-galaxies in the two richest ACO clusters in our catalog, A2840 (f_e = 21%) and A2860 (f_e = 19%)

7. Properties of galaxies in groups

In this section we examine the luminosities and the spectral features of galaxies in different environments: the "field", groups, and clusters. The dependence of these properties on the environment offers insights into the processes of galaxy formation and evolution and on the dynamical status of groups.

7.1. The luminosity function of members

Here we investigate the possible difference between the luminosity functions of member and non-member galaxies. We compute the luminosity function with the STY method (Sandage, Tamman & Yahil 1979). We assume a Schechter (1976) form for the luminosity function and follow the procedure described in detail in Zucca et al. (1997).

We find that galaxies in groups have a brighter M^* with respect to non–member galaxies; the slope α does not change significantly in the two cases. In particular the parameters we obtain are $\alpha = -1.25^{+0.11}_{-0.11}$ and $M^* = -19.80^{+0.14}_{-0.13}$ for the 1250 members, and $\alpha = -1.21^{+0.10}_{-0.09}$ and $M^* = -19.52^{+0.10}_{-0.10}$ for the 1835 non–members.

In Fig. 8 we draw (dotted lines) the confidence ellipses of the α and M^* parameters obtained in the two cases of member and non-member galaxies. The two luminosity functions differ at the 2σ level. In Fig. 8 we also plot the confidence ellipses for the parameters of the total sample (solid lines) derived in the same volume of ESP where we identify groups.

The fact that galaxies in groups are brighter than non-member galaxies is a clear demonstration of the existence of luminosity segregation in the ESP survey, a much deeper survey than those where the luminosity segregation has been previously investigated (Park et al. 1994, Willmer et al. 1998). Our finding is consistent with the results of Lin et al. (1996), who find evidence of a luminosity bias in their analysis of the LCRS power spectrum.

In further support of the existence of a luminosity segregation, we also find that M^* becomes brighter for members of groups of increasing richness. As before, the parameter α remains almost constant. Only in the case of the richest groups, $N_{mem} \geq 10$, we find a marginally significant steepening of the slope α.

7.2. Emission/absorption lines statistics

One interesting question is whether the environment of a galaxy has a statistical influence on the presence of detectable emission lines in the galaxy spectrum. Because emission lines galaxies are mostly spirals (Kennicutt 1992), the answer to this question is relevant to the investigation of the morphology-density relation in systems of intermediate density.

The fraction of ESP galaxies with detectable emission lines within the redshift range $5000 \leq cz \leq 60000\,\mathrm{km\,s^{-1}}$ is 44% (1360/3085). Of these $e.l.$-galaxies , (34 ± 2)% (467/1360) are members of groups. The fraction of galaxies without detectable emission lines, $a.l.$-galaxies , that are members of groups is significantly higher: 783/1725 or (45 ± 2)%. We note that our detection limit for emission lines correspond to an equivalent width of about 5 Å

Table 2. Frequency of Emission Line Galaxies in Different Environments

	$N_{e.l.}$	$N_{a.l.}$	N_{tot}
"field"	893	942	1835
rich groups	266	549	815
total	1159	1491	2650

We consider three types of environments: a) the "field", i.e. all galaxies that have not been assigned to groups, b) poor goups, i.e. groups with $3 \leq N_{mem} \leq 4$, and c) rich groups with $5 \leq N_{mem}$. We find that the fraction of $e.l.$-galaxies decreases as the environment becomes denser. In the "field" the fraction of $e.l.$-galaxies is f_e = 49%, it decreases to f_e = 46% for poor groups and to f_e = 33% for richer groups. In Fig. 9 we plot f_e as a function of N_{mem}. We also indicate the values of f_e of the two richest Abell clusters in our catalog, A2840 (f_e = 21%) and A2860 (f_e = 19%).

The significance of the correlation between environment and f_e can be investigated with a 2-way contingency table (Table 2). For simplicity, we do not consider triplets and quadruplets.

The contingency coefficient is C=0.15 and the significance of the correlation between environment and frequency of emission line galaxies exceeds the 99.9% level.

Our result indicates that the morphology-density relation extends over the whole range of densities from groups to clusters. Previous indications of the existence of the morphology-density relation for groups are based either on very local samples (Postman & Geller 1984) or on samples that are not suitable for statistical analysis (Allington-Smith et al. 1993). Very recently, Hashimoto et al. (1998) also confirm the existence of a morphology-density relation over a wide range of environment densities within LCRS.

Examining our result in more detail, we note that the fraction of $e.l.$-galaxies , f_e, in triplets and quadruplets is very similar to the value of f_e for isolated galaxies. Triplets and quadruplets are likely to correspond, on average, to the low-density tail of groups. Moreover, Ramella et al. (1997) and Frederic (1995a) estimate that the FOFA could produces a large fraction of unbound triplets and quadruplets. These "pseudo-groups" dilute the properties of real bound triplets and quadruplets with "field" galaxies, artificially increasing the value of f_e. This effect, in our survey, is partially counter-balanced by the triplets and quadruplets that are actually part of richer systems cut by the OPTOPUS mask. Considering that rich systems are significantly rarer than triplets and quadruplets, we estimate that the value of f_e we measure for triplets and quadruplets should be considered an upper limit.

Our catalog also includes ESP counterparts of 17 clusters listed in at least one of the ACO, ACOS (Abell et al. 1989) or EDCC (Lumsden et al. 1992) catalogs (Sect. 8, Table 3). For these clusters $f_{e,clusters}$ = 0.25 (63 $e.l.$-galaxies out of 256 galaxies). The number of members of these systems is not a direct measure of their richness because of the apparent magnitude limit of the catalog and because of the OPTOPUS mask. However, because they include all the richest systems in our catalog and because they are counterparts of 2-D clusters, it is resonable to assume that they are intrinsically rich. We remember here that Biviano et al. (1997) find f_e = 0.21 for their sample of ENACS clusters.The fact that for ESP counterparts of clusters we find a lower value of f_e than for the other rich groups ($f_{e,groups}$ = 0.36 without clusters), further supports the existence of a morphology-density relation over the whole range of densities from clusters to the "field".

Many systems of our catalog are not completely surveyed, therefore the relationship between f_e and the density of the environment we find can only be considered qualitative. However, while incompleteness certainly increases the variance around the mean result, we do not expect severe systematic biases. In order to verify that incompleteness does not affect our results, we consider the subsample of 67 groups that contain no ESP objects without measured redshift. We obtain for this subsample the same relationship between group richness and fraction of emission line galaxies we find for the whole catalog.

7.3. Seyfert galaxies

Within ESP we identify 12 Seyfert 1 galaxies and 9 Seyfert 2 galaxies. We identify type 1 Seyferts visually on the basis of the presence of broad (FWHM of a few 10^3 km s^{-1}) components in the permitted lines. Our list is complete with the possible exception of objects with weak broad lines which are hidden in the noise.

The identification of type 2 Seyferts is not straightforward, because it is based on line ratios and usually requires measurements of emission lines which fall outside our spectral range: only the F([O III]λ5007)/F(Hβ) ratio is available from our spectra, and it is therefore impossible to draw a complete diagnostic diagram (Baldwin et al. 1981, Veilleux & Osterbrock 1987). We classify tentatively as type 2 Seyferts all emission line galaxies with $\log(\mathrm{F([O\ III]}\lambda5007)/\mathrm{F(H}\beta)) \geq 0.7$: this threshold cuts out almost all non-active emission line galaxies, but also many narrow-line AGN with a medium to low degree of ionization. Thus the list of possible Seyfert 2 galaxies is almost free of contamination, but should by no means be considered complete.

The origin of the Seyfert phenomenon could be related to the interaction with close companions (Balick & Heckman 1982, Petrosian 1982, Dahari 1984, MacKenty 1989), or to a dense environment (Kollatschny & Fricke 1989, De Robertis et al. 1998). Observational evidence is, however, far from conclusive. For example, Seyfert 1 and Seyfert 2 galaxies have been found to have an excess of (possibly) physical companions compared to other spiral galaxies by Rafanelli et al. (1995). Laurikainen & Salo (1995) agree with Rafanelli et al. (1995) about Seyfert 2 galaxies, but reach the opposite conclusion about Seyfert 1 galaxies.

In our case, 7 (33%) out of 21 Seyferts are group members. For comparison, 460 (34%) emission line galaxies (not including Seyfert galaxies) are group members and 879 are either isolated or binaries. Clearly, within the limits of our relatively poor

statistics, we find that Seyfert galaxies do not prefer a different environment than that of the other emission line galaxies.

In order to test the dependence of the Seyfert phenomenon on the interaction of galaxies with close companions rather than with the general environment, we compute for all Seyferts and emission line galaxies the projected linear distance to their nearest neighbor, the nn-distance. We limit the search of companions to galaxies that are closer than 3000 km s^{-1} along the line of sight.

We find that the distribution of nn-distances of the sample of Seyfert galaxies is not significantly different from that of all emission line galaxies.

We also consider the frequency of companions at projected linear distances $d < 0.15h^{-1}$ Mpc. We have 7 Seyfert galaxies with such a close companion (33%) and 315 (23%) emission lines galaxies. One of the 7 Seyferts is a member of a binary systems, the remaining six Seyferts are members of groups. Even if, taken at face value, the higher frequency of close companions observed among Seyfert galaxies supports a causal connection between gravitational interaction and the Seyfert phenomenon, these frequencies are not significantly different.

We note that members of close angular pairs ($\theta < 24.6$ arcsec) in the original target list for ESP, are more frequently missing from the redshift survey than other objects (Vettolani et al. 1998). This bias, due to OPTOPUS mechanical constraints, could hide a possible excess of physical companions of Seyfert galaxies.

In order to estimate how strongly our result could be affected by this observational bias, we identify the nearest neighbors of Seyfert and emission line galaxies from a list including both galaxies with redshift and objects that have not been observed. When we compute projected linear distances to objects that have not been observed, we assume that they are at the same redshift of their candidate companion galaxy. As before, we do not find significant differences between the new nn-distributions of Seyferts and $e.l.$-galaxies .

This result demonstrates that the higher average incompleteness of close angular pairs does not affect our main conclusions: a) Seyfert galaxies within ESP are found as frequently within groups as other emission line galaxies, b) Seyfert galaxies show a small but not significant excess of close physical companions relative to the other emission line galaxies. We point out again that the sample of Seyferts is rather small and the statistical uncertainties correspondingly large.

8. Clusters and rich systems

Within our survey lie the centers of 9 ACO clusters, 5 ACOS clusters and 12 EDCC clusters. Several entries of the three lists correspond to the same cluster. Taking into account multiple identifications, there are 20 clusters listed within one or more of the three catalogs that lie within ESP.

In our catalog we find at least one counterpart for 17 out of the 20 clusters. The three clusters that do not correspond to any of our systems are ACO 2860, ACOS 11, and ACOS 32, all of Abell richness R = 0. ACO2860 is a very nearby object with a redshift, z = 0.0268, close to our minimum redshift. ACOS 11 and ACOS 32 are both distance class D = 6 objects that may be either projection effects or real clusters located beyond our redshift limit. We select the ESP counterparts among the groups that are close to the clusters on the sky and that have a redshift compatible with the distance class and/or magnitude of the cluster. If more ESP groups are counterparts of a cluster, we identify the cluster with the richest counterpart.

In Table 3 we list the name (column 1), and the coordinates (columns 4, 5) of the 17 clusters with ESP counterpart together with their richness (column 6) and, if available, their redshift as estimated by Zucca et al. (1993) (column 7). In the case of clusters listed in both EDCC and ACO or ACOS, we give the ACO or ACOS identification number. In the same Table 3 we also list the ID number of the cluster counterparts within our catalog (column 2), their number of members (column 3), redshift (column 8) and velocity dispersion (column 9).

There are 8 clusters with redshift estimated by Zucca et al. (1993) The measured redshifts of 6 of these clusters are in good agreement with the estimated redshift: the difference between the two redshifts is of the order of 10%, less than the 20% uncertainty on the estimated redshifts. For the remaining 2 clusters, ACO 2828 and ACO 4068, the estimated redshift is significantly smaller than our measured redshift. The projection of the foreground systems ESP 175 and ESP 178 within the Abell radius of ACO 2828 could explain the inconsistency between estimated and measured redshift for this cluster. In the case of ACO 4068 we do not find any foreground/background system within ESP. ACO 4068 is very close to the northern declination boundary of the ESP strip. An inspection of the COSMOS catalog just outside the boundary of the OPTOPUS field containing ACO 4068 shows that a significant part of this cluster lies outside our redshift survey and therefore background/foreground projection could still be the cause of the inconsistency between its estimated and measured redshifts.

We also note that EDCC163 and ACOS1055 are among the most incomplete systems in our catalog. In the fields of EDCC163 (N_{mem} = 3) and ACOS1055 (N_{mem} = 9) the number of objects without redshift is 16 and 63 respectively. We will not consider these two clusters in what follows.

In panel a) and panel b) of Fig. 10 we plot, respectively, N_{mem} and σ_{cz} as a function of cz. As expected, clusters (represented by large dots) populate the highest part of both diagrams at all redshifts. In both diagrams, mixed with clusters, there are also ESP groups that have not been identified as clusters.

The completeness of bidimensional cluster catalogs is an important issue for cosmology (van Haarlem et al. 1997) since the density of these clusters and their properties are used as constraints on cosmological models (e.g. Frenk et al. 1990, Bahcall et al. 1997, Coles et al. 1998). It is therefore interesting to determine whether there are other systems selected in redshift space that have properties similar to those of the cluster counterparts but that have escaped 2-D identification.

We limit our search for "cluster-like" groups to the velocity range $25000 < cz < 45000$ km s^{-1}. Within this range the selection function is rather stable and relatively close to its maximum.

Table 3. Clusters within ESP

ID	ESP	N_{mem}	α_{1950} ($^h\ ^m\ ^s$)	δ_{1950} (^{o} ' ")	R	z_{est}	z_{ESP}	σ km s^{-1}
E0163	6	3	22 32 40	−40 38 41			0.13535	121
E0169	7	11	22 34 12	−39 50 51			0.06294	282
S1055	21	9	22 39 43	−40 16 07	0		0.02901	102
A4068	88	9	23 57 08	−39 46 59	0	0.07151	0.10261	700
E0435	121	8	00 17 31	−40 40 37			0.15073	334
A2769	126	6	00 21 45	−39 53 49	0	0.15708	0.14020	419
A2771	128	18	00 21 50	−40 26 49	0	0.06260	0.06876	268
A2828	176	5	00 49 10	−39 50 54	0	0.13133	0.19676	468
A2840	183	34	00 52 01	−40 04 19	1	0.10460	0.10618	339
A2852	192	12	00 57 00	−39 54 19	0	0.17581	0.19845	235
E0113	196	16	00 58 21	−40 31 05			0.05449	372
A2857	200	8	01 00 06	−40 12 42	1	0.19092	0.19755	504
E0519	205	43	01 02 36	−40 03 02			0.10637	319
S0127	213	25	01 05 27	−40 21 08	0		0.10498	505
A2874	216	25	01 06 08	−40 36 01	1	0.15812	0.14191	817
E0529	218	17	01 07 40	−40 40 34			0.10483	282
E0546	231	7	01 19 27	−39 53 07			0.11909	424

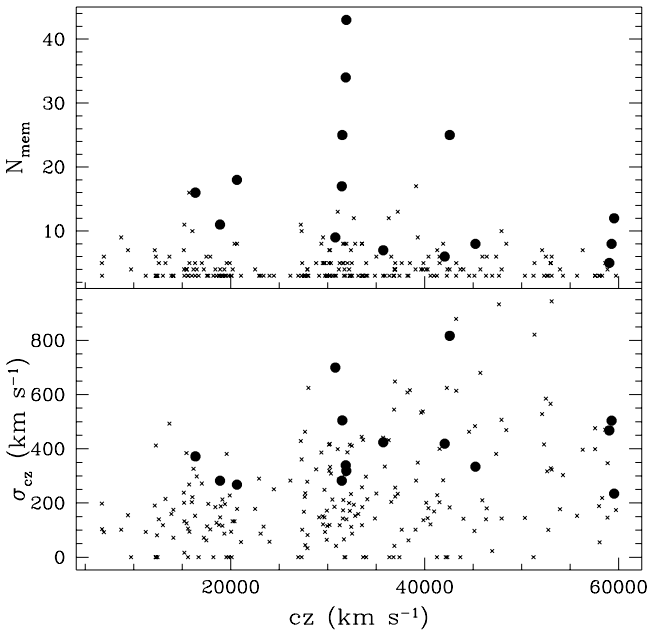

Fig. 10. N_{mem} (*top panel*) and σ_{cz} (*bottom panel*) as a function of cz. Large dots are ESP counterparts of 2-D ACO and/or EDCC catalogs.

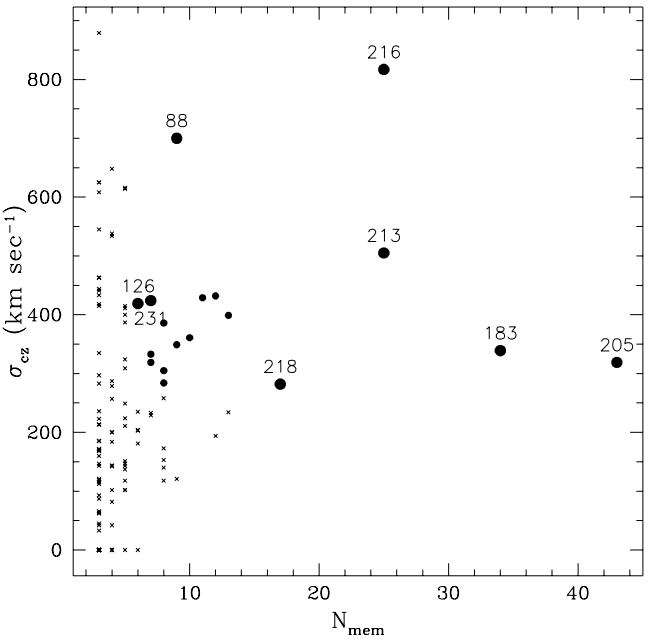

Fig. 11. ESP groups (crosses) with 25000 km s^{-1} $< cz <$ 45000 km s^{-1} in the σ_{cz}– N_{mem} plane. Large dots are ESP counterparts of 2-D ACO and/or EDCC catalogs, smaller dots are "cluster-like" groups. The ESP counterparts of ACO and/or EDCC clusters are labeled with their ESP ID number (Table 1).

In our catalog we identify the counterparts of 8 2-D clusters within this redshift range. Two of the eight clusters are of richness class R=1 (ACO2840=ESP183 and ACO2874=ESP216). The minimum number of members of these clusters is 6 and the lowest velocity dispersion of the 8 clusters is 280 km s^{-1}.

Apart from the counterparts of the 8 clusters, we find 11 additional ESP groups that satisfy all three conditions $25000 < cz < 45000$ km s^{-1}, $N_{mem,min} \geq 6$, and $\sigma_{cz,min} \geq 280$ km s^{-1}. These groups are $\simeq$ 10% of all groups in this redshift interval and we list them in Table 4.

In a σ_{cz}– N_{mem} plane, Fig. 11, the eleven "cluster-like" groups occupy a "transition region" between clusters and groups. First we note that, in this plane, the two counterparts of the R=1 ACO clusters (ESP183 and ESP216) are very distant from the "cluster-like" groups. The same holds true for the only rich EDCC cluster that is not an ACO cluster, EDCC519. We conclude that no rich cluster is missing from 2-D catalogs in the

Table 4. Cluster-like groups

ESP	N_{mem}	α_{1950} $h\ m\ s$	δ_{1950} $^o\ '\ ''$	cz km s^{-1}	σ km s^{-1}
48	7	23 26 03	−39 52 45	30231	333
96	8	00 02 04	−40 29 17	29329	386
124	17	00 20 33	−40 33 37	39102	283
130	8	00 23 02	−40 15 47	41898	284
155	9	00 40 39	−40 00 46	39280	349
186	7	00 54 16	−40 25 00	30163	319
190	13	00 55 29	−40 34 41	31033	399
195	8	00 58 10	−40 06 00	31728	305
201	11	01 00 34	−40 03 30	27225	429
203	10	01 02 28	−40 18 29	27298	361
226	12	01 14 57	−39 52 45	36298	432

region of the sky covered by the ESP survey. This conclusion is reassuring, even if it does not allow us to discuss the problem of the completeness of rich 2-D clusters in general because it is based on a small number of objects.

In the case of the more numerous poorer clusters, Fig. 11 shows that several systems could be missing from the 2-D list. The boundaries of the cluster and group regions in the σ_{cz}–N_{mem} plane are blurred by the OPTOPUS mask and by the narrow width of the ESP survey. It is therefore difficult to give a precise estimate of how many "cluster-like" groups should be considered "missing" from bidimensional catalogs.

That poor 2-D clusters and "cluster-like" 3-D groups are probably the same kind of systems is confirmed by the fact that they have the same fraction of $e.l.$-galaxies , a higher value than it is typical of richer clusters. The 11 "cluster-like" groups have a total of 110 members, 43 of which are $e.l.$-galaxies : $f_{e,cluster-like}$ = 0.39. The 4 poor clusters that have $N_{mem} \leq$ 17 include 39 members and have $f_{e,poor\ clusters}$ = 0.41. We remember here that for all ESP counterparts of clusters we find $f_{e,clusters}$ = 0.25.

In conclusion, the comparison of ESP systems with ACO, ACOS and EDCC clusters indicates that the "low mass" end of the distribution of clusters is poorly represented in 2-D catalogs; on the other hand, the 2-D catalogs appear reasonably complete for high mass clusters.

9. Summary

In this paper we search objectively and analyze groups of galaxies in the recently completed ESP survey ($23^h23^m \leq \alpha_{1950} \leq 01^h20^m$ and $22^h30^m \leq \alpha_{1950} \leq 22^h52^m$; $-40^o45' \leq \delta_{1950} \leq -39^o45'$). We identify 231 groups above the number overdensity threshold $\delta\rho/\rho$ =80 in the redshift range 5000 km s^{-1} $\leq cz \leq$ 60000 km s^{-1}. These groups contain 1250 members, 40.5% of the 3085 ESP galaxies within the same cz range. The median velocity dispersion of ESP groups is $\sigma_{ESP,median}$ = 194 km s^{-1} (at the redshift of the system and taking into account measurement errors). We verify that our estimates of the average velocity dispersions are not biased by the geometry of the ESP survey which causes most systems to be only partially surveyed.

The groups we find trace very well the geometry of the large scale distribution of galaxies, as they do in shallower surveys. Because groups are also numerous, they constitute an interesting characterization of the large scale structure. The following are our main results on the properties of groups that set interesting "constraints" on cosmological models:

- the ratio of members to non-members is $f_{ESP,mem}$ = 0.68 $\pm$ 0.02. This value is in very close agreement with the value found in shallower surveys, once the few richest clusters (e.g. Coma and Virgo) are neglected.
- the ratio of groups to the number of non-member galaxies is $f_{ESP,groups}$ = 0.13 $\pm$ 0.01, also in very close agreement with the value found in shallower surveys.
- the distribution of velocity dispersions of ESP groups is not distinguishable from those of CfA2N and SSRS2 groups.

These results are of particular interest because the ESP group catalog is five times deeper than any other wide-angle shallow survey group catalog and the number of large scale features explored is correspondingly larger. As a consequence, the properties of ESP groups are more stable with respect to possible structure-to-structure variations. The fact that the properties of ESP groups agree very well with those of CfA2N and SSRS2 groups indicates that structure-to-structure variations are not large and that the properties of groups we find can be considered representative of the local universe.

As far as the richest systems (clusters) are concerned, we identify ESP counterparts for 17 out of 20 2-D selected ACO and/or EDCC clusters. Because the volume of ESP is comparable to the volume of individual shallower surveys, it is not big enough to include a fair sample of clusters. The variations from survey to survey in the number and properties of clusters are large.

Turning our attention to properties of galaxies as a function of their environment, we find that:

- the Schechter luminosity function of galaxies in groups has a brighter M^* (-19.80) with respect to non–member galaxies ($M^* = -19.52$); the slope α ($\simeq$ 1.2) does not change significantly between the two cases.
- M^* becomes brighter for members of groups of increasing richness. The parameter α remains almost constant; only in the case of the richest groups we find a marginally significant steepening of the slope α.
- 34% (467/1360) of ESP galaxies with detectable emission lines are members of groups. The fraction of galaxies without detectable emission lines in groups is significantly higher: 45% (783/1725).
- the fraction of $e.l.$-galaxies in the field is f_e = 49%; it decreases to f_e = 46% for poor groups and to f_e = 33% for richer groups. For the ESP counterparts of ACO and/EDCC clusters f_e = 25%.

We conclude that luminosity segregation is at work in the ESP survey: galaxies in the dense environment of groups are, on

average, brighter than "field" galaxies. Galaxies in groups are also less likely to have detectable emission lines in their spectra. In fact, we find a gradual decrease of the fraction of emission line galaxies among members of systems of increasing richness: the morphology-density relation clearly extends over the whole range of densities from groups to clusters.

As a final note, we identify 12 Seyfert 1 galaxies and 9 Seyfert 2 galaxies. We find that: a) Seyfert galaxies within ESP are members of groups as frequently as other emission line galaxies, and b) Seyfert galaxies show a small but not significant excess of close physical companions relative to the other emission line galaxies. We point out again that the sample of Seyferts is rather small and the statistical uncertainties correspondingly large.

Acknowledgements. We thank the referee for his careful reading of the manuscript and his helpful suggestions. This work has been partially supported through NATO Grant CRG 920150, EEC Contract ERB–CHRX–CT92–0033, CNR Contract 95.01099.CT02 and by Institut National des Sciences de l'Univers and Cosmology GDR.

References

Abell G.O., Corwin Jr. H.G., Olowin R.P., 1989, ApJS 70, 1 (ACO, ACOS).
Allington-Smith J.R., Ellis R., Zirbel E.L., Oemler A. Jr., 1993, ApJ 404, 521.
Bahcall N.A., Fan X., & Cen R., 1997, ApJL 485, 53.
Baldwin J.A., Phillips M.M., & Terlevich R., 1981, PASP, 93, 5.
Balick B., & Heckman T.M., 1982, ARA&A 20, 431.
Biviano A., Katgert P., Mazure A. et al., 1997, A&A 321, 84.
Coles P., Pearson R.C., Borgani S., Plionis M., & Moscardini L., 1998, MNRAS 294, 245.
da Costa L.N., Geller M.J., Pellegrini P.S. et al. 1994, ApJ 424, L1.
Dahari O., 1984, AJ 89, 966.
Danese L., De Zotti G., & di Tullio G., 1980, A&A 49, 137.
Davis, M., & Huchra, J.P., 1982, ApJ 254, 437.
De Robertis M.M., Yee H.K.C., & Hayhoe K., 1998, ApJ 496, 93.
Dressler A., 1980,ApJ 236, 351.
Frenk C.S., White S.D.M., Efstathiou G., & Davis M., 1990, ApJ 351, 10.
Frenk C.S., Evrard A.E., White S.D., & Summers F.J., 1996, ApJ 472, 460.
Frederic, J.J., 1995a, ApJS, 97, 259.
Frederic, J.J., 1995b, ApJS, 97, 275.
Geller M.J., & Huchra J.P., 1989, Science 246, 897.
Hashimoto Y., Oemler A. Jr., Lin H., & Tucker D.L., 1998, ApJ 499, 589.
Heydon–Dumbleton N.H., Collins C.A., MacGillivray H.T., 1988, in *Large–Scale Structures in the Universe*, ed. W. Seitter, H.W. Duerbeck and M. Tacke (Springer–Verlag), p. 71.
Heydon–Dumbleton N.H., Collins C.A., MacGillivray H.T., 1989, MNRAS 238, 379.
Huchra J.P., & Geller M.J., 1982, ApJ 257, 423.
Kaufmann G., Nusser A., & Steinmetz M., 1997, MNRAS 286, 695.
Kennicutt R.C. Jr., 1992, Apj 388, 310.
Kollatschny W., & Fricke K.J., 1989, A&A 219, 34.
de Lapparent V., Geller M.J., & Huchra J.P., 1988, ApJ 332, 44.
Laurikainen E., & Salo H., 1995, A&A 293, 683.
Ledermann W., 1984, *Handbook of Applicable Mathematics* (Wiley and Sons), Vol. VI, part A.
Lin H., Kirshner R.P., Shectman S.A., Landy S.D., Oemler A Jr., Tucker D.L., & Schechter P.L., 1996 ApJ 471, 617.
Lumsden S.L., Nichol R.C., Collins C.A., Guzzo L., 1992, MNRAS 258, 1 (EDCC).
MacKenty J.W., 1989, ApJ 343, 125.
Marzke R.O., Geller M.J., da Costa L.N., & Huchra J.P., 1995, AJ 110,477.
Mattig W. 1958, Astron. Nachr. 284, 109.
Moore B., Frenk C.S., & White S.D.M., 1993, MNRAS 261, 827.
Nolthenius R, Klypin A.A., & Primack J.R., 1994, ApJ 422, L4
Nolthenius R, Klypin A.A., & Primack J.R., 1997, ApJ 480,43.
Park C., Vogeley M.S., Geller M.J., & Huchra J.P., 1994, ApJ 431, 569.
Petrosian A.R., 1982, Astrophysics 18, 312.
Postman M., & Geller M.J., 1984, ApJ 281, 95.
Rafanelli P., Violato M., Baruffolo A., 1995, AJ 109,1546.
Ramella M., Geller M.J., & Huchra J.P., 1989, ApJ 344, 57.
Ramella M., Geller M.J., & Thorstensen J., 1995, AJ 109, 1469.
Ramella M., Focardi P., & Geller M.J., 1996, A&A 312, 475.
Ramella M., Pisani A., & Geller M.J., 1997, AJ 113, 483 (RPG).
Ramella M. et al. 1998, in preparation.
Sandage A., Tamman G., & Yahil A., 1979, ApJ 232, 252.
Schechter P., 1976, ApJ 203, 297.
Shectman S.A., Landy S.D., Oemler A. et al. 1996, ApJ 470, 172 (LCRS).
Trasarti-Battistoni R., 1997, A&ASS 130, 341.
Tucker D.L., Hashimoto Y., Kirshner R.P. et al. 1997, astro-ph 9711176.
van Haarlem M.P., Frenk C.S., & White S.D., 1997, MNRAS 287, 817.
Veilleux S., & Osterbrock D.E., 1987, ApJS 63, 295.
Vettolani G., Zucca E., Zamorani G. et al. 1997, A&A 325, 924.
Vettolani G., Zucca E., Merighi R. et al. 1998, A&ASS 130, 323.
Weinberg D.H., & Cole S., 1992, MNRAS 259, 652.
Willmer C.N.A., da Costa L.N., & Pellegrini P.S., 1998, AJ 115, 869.
Zabludoff A.I., Geller M.J., Huchra J.P., & Ramella M., 1993, AJ 106, 1301.
Zabludoff A.I., & Geller M.J., 1994, AJ 107, 1929.
Zucca E., Zamorani G., Vettolani G et al.., 1997, A&A 326, 477.
Zucca E., Zamorani G., Scaramella R., & Vettolani G., 1993, ApJ 407, 470.